IJE TRANSACTIONS A: Basics Vol. 28, No. 7, (July 2015) 1068-1073

International Journal of Engineering

Journal Homepage: www.ije.ir

Effect of Micellization pH on Properties of Sphere-like Mesoporous Hydroxyappatite

L. Bakhtiari*[,a], H. R. Rezaie[a], J. Javadpour[a], M. Erfan[b], M. A. Shokrgozar[c]

[a]*School of Metallurgical and Materials Engineering, Iran University of Science and Technology, Tehran, Narmak , Iran.*
[b]*School of Pharmacy, Shahid Beheshti University of Medical Sciences, Tehran, Iran.*
[c]*National Cell Bank of Iran, Pasteur Institute of Iran, Tehran, Iran*

PAPER INFO

Paper history:
Received 19 November 2014
Received in revised form 09 June 2015
Accepted 11 June 2015

Keywords:
Mesoporous
Hydroxy Appatite
Micellization pH
Sphere-like

ABSTRACT

Mesoporous hydroxyapatites were syntesized by self-assembly method using Cetyltrimethylammonium bromide (CTAB) as cationic surfactant and 1-dodecanethiol as pore expander with pore expander/surfactant mass ratio of 4.22 and synthesis temperature of 80 °C at different micellization pH values. The field emission-scanning electron microscopy (FESEM), X-ray diffraction (XRD), Brunauer-Emmett-Teller (BET) surface area analysis, pore size distribution plot (Barrettt, Joyner, and Halenda (BJH) method), fourier transform infrared spectroscopy (FTIR) and low-angle X-ray diffraction (LA-XRD) results beside the titration investigation of 1-dodecanethiol revealed that ionizied 1-dodecanethiol concentration ($[RS^-]$) increased exponentially by changes in pH. The micellization pH has a key role in physico-chemical characteristics of samples. Increase in pH can change the ionization degree of 1-didecanethiol and swell the micelle and also lead to larger pores (pore diameter of 2.93 in lower pH and 24.48 in higher pH). Changes in the micellization pH also affect the dielectric constant of water and lead to variation in patricle size.

***doi**: 10.5829/idosi.ije.2015.28.07a.13*

1. INTRODUCTION

Sphere-like porous hydroxyappatite with different properties has been synthesized by various methods. Immersion of glass spherical particles in phosphate solutions [1–5], solvothermal [6, 7], spray drying [8, 9], centrifugal spray drying [10], self-assmbly using hard template (chitin) [11] and self-assembly using soft templates (surfactants and block-copolymers) [6, 10], [12–19] are different methods that have been applied in the synthesis of sphere-like mesoporous hydroxyappatite. High degree of agglomeration, irregular morphology and size distribution, low pore volume and surface area are the major obstacles in synthesis of this biomaterial using soft template route and especially cationic surfactants. In order to overcome these problems and to further improve bioavailability of sphere-like mesoporous hydroxyappatite, development of this structure with uniform morphology, high surface area and pore volume is necessary.

Among a few studies on sphere-like mesoporous hydroxyapatite synthesized with CTAB as cationic surfactant [20, 21], there is no study on synthesis parameteres of mesoporous hydroxyappatite with cationic surfactants in the presence of 1-dodecanethiol as pore expander. In this study, one of the main synthesis parameteres of mesoporous hydroxyappatite, the micellization pH, was investigated.

2. MATERIALS AND METHOD

All materials; cetyltrimethylammonium bromide (CTAB), sodium hydroxide (NaOH), 1-dodecanethiol (C_{12}-SH), calcium nitrate (Ca $(NO_3)_2.4H_2O$), ortho phosphoric acid (85% purity) and ammonia solution (25% extra pure) were purchased from Merck.

In a typical proceudre, emulsion of CTAB and 1-dodecanethiol (1-dodecanethiol/surfactant mass ratio of

*Corresponding Author's Email: Lbakhtiari@iust.ac.ir (L. Bakhtiari)

Please cite this article as: L. Bakhtiari, H. R. Rezaie, J. Javadpour, M. Erfan, M. A. Shokrgozar, Effect of Micellization pH on Properties of Sphere-like Mesoporous Hydroxyappatite, International Journal of Engineering (IJE), TRANSACTIONS A: Basics Vol. 28, No. 7, (July 2015) 1068-1073……

4.22) with adequate amount of NaOH solution (2M) in 100 ml deionized water were stirred under magnetic stirrer at 80 ºC for 30 min. Precursors of hydroxyapatite were dissolved in equal volume of deionized water (0.01 mole calcium nitrate and 0.006 mole ortho phosphoric acid). The prepared solutions were quickly added to above solution and stirred for 2 h. The pH of solution was adjusted by ammonia solution at 11 for H1 sample and 13 for H2 sample. The white precipitation was filtered, washed and then dried at 60 ºC overnight. The final powder was calcined at 550 ºC for 5 h at a heating rate of 1 ºC/min.

The presented crystalline phases were determined by using X-ray diffraction (XRD: JDX-8030, Jeol, Japan). The extension of ordering in the pore structure was investigated using low angle X-ray diffraction (LA-XRD) (PANalytical, X'Pert PRO MPD). Fourier transform infrared spectroscopy (FTIR) was used for further investigation (Shimadzu, 8400s). The morphology of the samples was investigated by field emission scanning electron microscopy (FESEM: Hitachi, S4160). The Brunauer-Emmett-Teller (BET) specific surface areas were determined by Bellsorp mini-II /Japan. The titration investigation was carried out by BEL pH-meter (Italy).

3. RESULTS AND DISCUSSION

3. 1. Phase Dentification The XRD patterns of different synthesized hydroxyapatite samples are shown in Figure 1. All the peaks correspond to the stoichiometric hydroxyapatite (PDF file no. 09-0432) in the ICDD data base [22]. There was no difference between H1 and H2 sample ptterns which have been synthesized under different micellization pH values. This can be explained by this matter that changes in the micellization pH can only affect the template (micelle) form and not the final hydroxyapatite phase. Other analysis prove this point as it will be mentioned as follows.

Figure 2 shows two calcined samples and also CTAB and 1-dodecanethiol spectra. As can be seen, all characteristic bands of hydroxyapatite structure (PO_4^{-3} group at 570 and 1047 cm^{-1}, CO_3^{-2} group in the range of 1400-1500 cm^{-1}, absorbed water at about 3000 cm^{-1} and hydroxyl group at about 3300 cm^{-1}) [23] are observable in spectra. Characteristic peaks of CTAB and 1-dodecanethiol are not seen in H1 and H2 samples. This can be approved the complete removal of these materials after calcination procedure.

3. 2. Morphology and Pore Characteristics Figure 3 shows the FESEM micrographs of samples. The microscope working voltage was 15 kV and the secondary image type was selected for microscopy images. The powder products were dispersed in ethanol by sonication for 10 min, put on a carbon wafer. The white powders were coated with a layer of gold before FESEM observations. Both samples showed spherical particles with different particle sizes. It can be deduced that by increasing the micellization pH, a decrease in particle size occurred. Increase in pH reduces the CMC value for the micelle formation due to increase in the ionic strength of the system. This can increase the aggregation number of the micelle (Nagg) and decrease the degree of counterion dissociation (β: the degree of counterion dissociation).

The ions of C_{12}-SH molecule (C_{12}-S^- and H^+) and counterions of CTAB (Br^-) and sodium hydroxide ions (Na^+ and OH^-) present in the sol. Increase in pH will increase the OH^- ions in the sol which can act both as a helping factor in ionization of swelling agent (C_{12}-SH) and also reduce the stability of dissociated ions. More OH^- ions can interact with H^+ to produce H_2O molecule and thus increase the ionization of swelling agent.

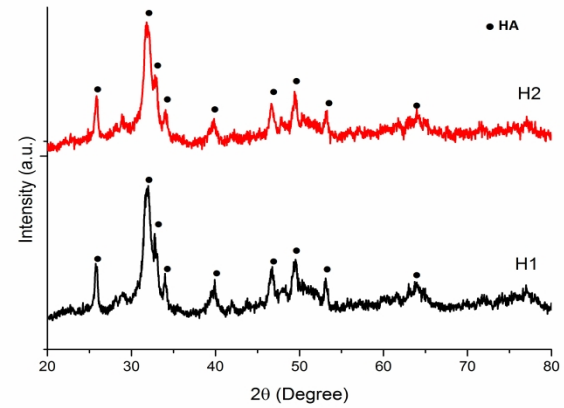

Figure 1. XRD patterns of synthesized samples

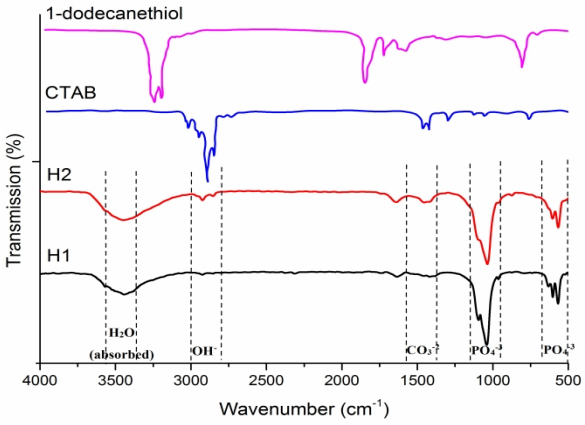

Figure 2. FTIR spectra of the indicated samples.

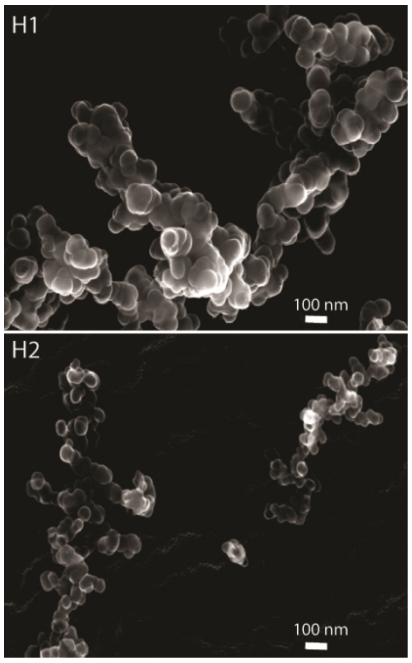

Figure 3. FESEM micrographs of H1 sample (synthesized at pH=11) and H2 sample (synthesized at pH=13).

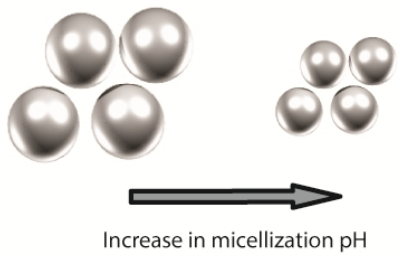

Figure 4. Schematic illustration of morphological changes by increase in micellization pH.

Na^+ ions react with counterions of CTAB (Br^-) and produce NaBr molecule which are removed in the washing process. In other words, increase in pH reduces the stability of dissociated ions reducing the dielectric constant of solvent (water) [22, 23]. Decrease in dielectric constant of water will increase the repulsive force and decrease the size of sphere-like particles [26]. Schematic illustration of changes in particle size is shown in Figure 4. Figure 5 shows nitrogen adsorption-desorption isotherms for the calcined samples. Hystersis loops of samples are different. H1 sample, which synthesized under low micellization pH, shows narrow hystersis loop in comparision with H2 sample. Pore size distribution plots of samples which meseared by BJH method, are presented in Figure 6. It can be seen that H2 sample has larger pore distribution. Table 1 summarizes the physical characteristics of different samples. As indicated in Table 1, the lower micellization pH, will reduce the pore volume, BET surface area and pore size diameter. This can be attributed to changes in ionization degree of 1-dodecanethiol as a function of pH. Increase in pH, can affect the ionization degree of swelling agent and help the micelle to swelle more and more. Electrostatic interaction between CTA^+ of CTAB and ionized 1-dodecanethiol (C_{12}-S^- ions) can form a swelled micelle which can result in high BET surface area, pore volume and pore diameter size [27].

To explore this phenomenon, ionization behavior of 1-dodecanethiol at synthesis temperature was investigated by titration of 1-dodecanethiol and NaOH solution (2M). Results of titration is presented in Figure 7 (part A). The changes of ionized 1-dodecanethiol as a function of pH is also presented in part B of Figure 7. General form of 1-dodecanethiol (RSH) is used for equations.

TABLE 1. Pore characteristics of calcined samples.

Sample code	BET surface area (m^2/g)	Pore volume (cm^3/g)	Pore size diameter (nm)
H1	106.63	0.079	3.42
H2	78.99	0.762	24.48

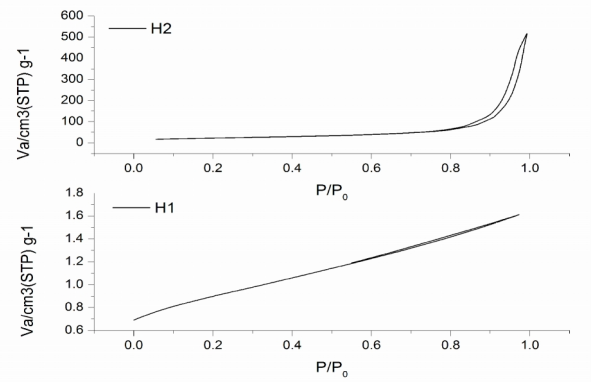

Figure 5. Nitrogen adsorption-desorption isotherms of indicated samples.

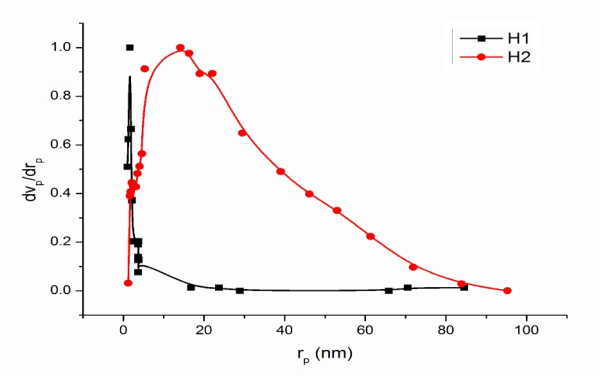

Figure 6. Corresponding pore size distribution obtained from samples.

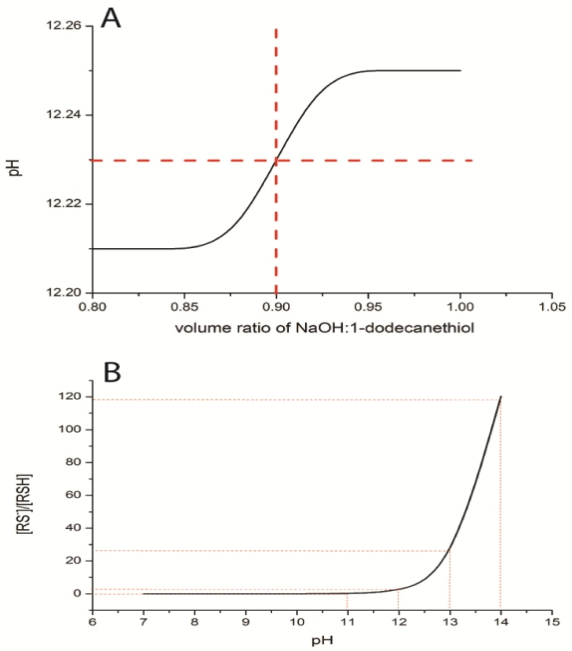

Figure 7. Titration graph of 1-dodecanethiol (A) and changes of ionized 1-dodecanethiol as a function of micellization pH (B).

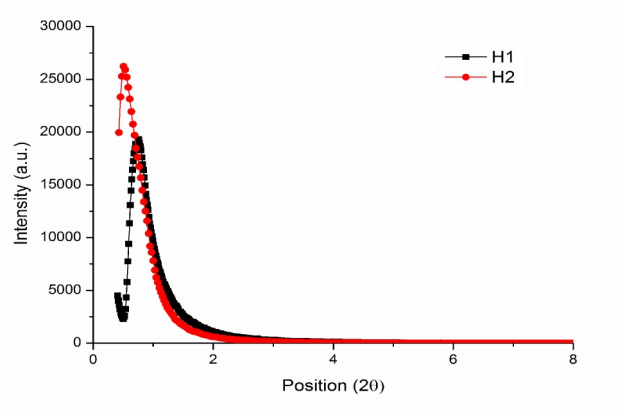

Figure 8. LA-XRD profiles of indicated samples.

TABLE 2. Pore characteristics of samples.

Sample code	d spacing (nm)*	a (nm)**	dp (nm)***
H1	13.049	15.352	3.42
H2	15.48	17.87	24.48

**d spacing* in low angle range corresponds to the distance between crystallographic sheets.
*** a* corresponds to the distance between the neighboring pore centers which is determined by $a = \frac{2d}{\sqrt{3}}$ in 2D hexagonal close packed pore structure [17].
**** dp*, pore diameter, is calculated from the adsorption branch of the isotherm using BJH method.

The shown diagram (part B) was extracted from the following equations [28]:

$$RSH \leftrightarrow RS^- + H^+ \quad (1)$$

$$Ka = \frac{H+ [RS-]}{[RSH]} \quad (2)$$

$$Ka = 10^{-pka} \quad (3)$$

$$\frac{[RS-]}{[RSH]} = 10^{(pH-11.92)} \quad (4)$$

As can be seen in Figure 7, complete ionization pH of 1-dodecanethiol occurs at pH~12.23 (equivalent point of titration graph). In analytical chemistry, Ka is known as acid ionization constant but its logarithmic measure is more commonly used which is known as pKa. The half-life of complete ionization in titration graph can be used in the determination of the pKa value (pKa =11.92). So due to Equation (4), $[RS^-]/[RSH]$ ratio grows exponentially by one unit changes in pH. So it can be concluded from above mentioned explanations that one unit change in pH, in a constant concentration of 1-dodecanethiol will cause ten times growth in anion concentration ($[RS^-]$) and more swelling of the micelle. LA-XRD profiles of samples are presented in Figure 8. It can be observed that decrease in micellization pH, can have a reducing effect on LA-XRD intensity. In the other words, increase in micellization pH can increase the partial degree of ordering in mesostructure.

Table 2 summarizes the pore characteristics of two samples. Details of Table 2 reveal that increase in micellization pH, can affect the *a* value (distance between pore centeres) and also the *d spacing* (distance of crystallographic sheets). Higher ionization degree of swelling agent and higher pH values can cause an increase in pore size diameter and *a* value.

4. CONCLUSIONS

In this study, we compared characteristics of sphere-like particles of mesoporous hydroxyappatite synthesized under different micellization pH in presence of 1-dodecanethiol as swelling agent and CTAB as cationic surfactant. Results of analysis revealed that there is an optimum amount of micellization pH to obtain proper mesostructure. On the other hand, increase in micellization pH can decrease the mesoporous nanoparticle size which is attributed to the reduction in repulsive force between the micelles. Beside the mentioned changes, increase in micellization pH can introduce more ionized 1-dodecanethiol which results in more swelling of the micelle and larger pore sizes. Increase in micelle size resulted in lower degree of ordering in meso structure. It can be concluded that the micellization pH, as a synthesis parameter, has a key

role in final properties of sphere-like mesoporous hydroxyappatite.

5. REFERENCES

1. W. Xiao, H. Fu, M. N. Rahaman, Y. Liu, and B. Sonny Bal, "Hollow hydroxyapatite microspheres: a novel bioactive and osteoconductive carrier for controlled release of bone morphogenetic protein-2 in bone regeneration," ***Acta Biomaterials***, Vol. 9, No. 9 (2013), 8374–8383.
2. Y. Wang, A. Yao, W. Huang, and D. Wang, "In situ fabrication of hollow hydroxyapatite microspheres by phosphate solution immersion," ***Journal of Crystal Growth***, Vol. 327, No. 1, (2011), 245–250.
3. H. Fu, M. N. Rahaman, D. E. Day, and R. F. Brown, "Hollow hydroxyapatite microspheres as a device for controlled delivery of proteins," ***Journal of Materials Science: Materials in Medicine.***, Vol. 22, No. 3, (2011), 579–591.
4. H. Fu, M. N. Rahaman, and D. E. Day, "Effect of process variables on the microstructure of hollow hydroxyapatite microspheres prepared by a glass conversion method," ***Journal of American Ceramic Society***, Vol. 93, No. 10, (2010), 3116–3123.
5. H. Fu, M. N. Rahaman, R. F. Brown, and D. E. Day, "Evaluation of BSA protein release from hollow hydroxyapatite microspheres into PEG hydrogel," ***Materials Science and Engineering C***, Vol. 33, No. 4, (2013), 2245–2250.
6. X. Zhang, W. Zhang, Z. Yang, and Z. Zhang, "Nanostructured hollow spheres of hydroxyapatite: preparation and potential application in drug delivery," ***Frontiers of Chemical Science and Engineering***, Vol. 6, No. 3, (2012), 246–252.
7. D. Gopi, J. Indira, L. Kavitha, M. Sekar, and U. K. Mudali, "Synthesis of hydroxyapatite nanoparticles by a novel ultrasonic assisted with mixed hollow sphere template method.," ***Spectrochimica Acta Part A: Molecular and Biomolecular Spectroscopy***, Vol. 93, (2012), 131–134.
8. R. Sun, K. Chen, and Y. Lu, "Fabrication and dissolution behavior of hollow hydroxyapatite microspheres intended for controlled drug release," ***Materials Reserach Bulletin*****,** Vol. 44, No. 10, (2009), 1939–1942.
9. R. Sun, Y. Lu, and K. Chen, "Preparation and characterization of hollow hydroxyapatite microspheres by spray drying method," ***Materials Science Engineering C***, Vol. 29, No. 4, (2009), 1088–1092.
10. Y. Jiao, Y.-P. Lu, G. Y. Xiao, W. H. Xu, and R. F. Zhu, "Preparation and characterization of hollow hydroxyapatite microspheres by the centrifugal spray drying method," ***Powder Technology***, Vol. 217, (2012), 581–584.
11. C. X. Jiang, B. Feng, S. X. Qu, L. Ming, J. Weng, and Q. Peng, "Preparation and characterization of hydroxyapatite microspheres with hollow core and mesoporous shell," ***Key Engineering Materials***, Vol. 309, (2006), 65–68.
12. Y. Mizushima, T. Ikoma, J. Tanaka, K. Hoshi, T. Ishihara, Y. Ogawa, and A. Ueno, "Injectable porous hydroxyapatite microparticles as a new carrier for protein and lipophilic drugs.," ***Journal of Controlled Release***, Vol. 110, No. 2, (2006), 260–265.
13. P. Shanthi, R. V Mangalaraja, A. P. Uthirakumar, S. Velmathi, T. Balasubramanian, and M. Ashok, "Synthesis and characterization of porous shell-like nano hydroxyapatite using Cetrimide as template," ***Journal of Colloid and Interface Science***, Vol. 350, No. 1, (2010), 39–43.
14. H. Wang, L. Zhai, Y. Li, and T. Shi, "Preparation of irregular mesoporous hydroxyapatite," ***Materials Reserch Bulletin***., Vol. 43, No. 6, (2008), 1607–1614.
15. Y. Dou, S. Cai, X. Ye, G. Xu, H. Hu, and X. Ye, "Preparation of mesoporous hydroxyapatite films used as biomaterials via sol–gel technology," ***Journal of Sol-Gel Science and Technology***, Vol. 61, No. 1, (2011), 126–132.
16. W. He, Z. Li, Y. Wang, X. Chen, X. Zhang, H. Zhao, S. Yan, and W. Zhou, "Synthesis of mesoporous structured hydroxyapatite particles using yeast cells as the template.," ***Journal of Materials Science: Materials in Medicin***, Vol. 21, No. 1, (2010), 155–159.
17. Y. Li, W. Tjandra, and K. C. Tam, "Synthesis and characterization of nanoporous hydroxyapatite using cationic surfactants as templates," ***Materials Research Bulletin***, Vol. 43, No. 8–9, (2008), 2318–2326.
18. G. K. Lim, J. Wang, S. C. Ng, and L. M. Gan, "Formation of Nanocrystalline Hydroxyapatite in Nonionic Surfactant Emulsions," ***Society***, No. 17, (1999), 7472–7477.
19. P. M. S. L. Shanthi, R. V Mangalaraja, a P. Uthirakumar, S. Velmathi, T. Balasubramanian, and M. Ashok, "Synthesis and characterization of porous shell-like nano hydroxyapatite using cetrimide as template.," ***Journal of Colloid and Interface Science***, Vol. 350, No. 1, (2010), 39–43.
20. M. Sadat-Shojai, M.-T. Khorasani, and A. Jamshidi, "Hydrothermal processing of hydroxyapatite nanoparticles—A Taguchi experimental design approach," ***Journal of Crystal Growth***, Vol. 361, (2012), 73–84.
21. Q. Zhao, T. Wang, J. Wang, L. Zheng, T. Jiang, G. Cheng, and S. Wang, "Fabrication of mesoporous hydroxycarbonate apatite for oral delivery of poorly water-soluble drug carvedilol," ***Journal of Non Crystal Solids***, Vol. 358, No. 2, (2012), 229–235.
22. N. Pramanik, T. Imae "Fabrication and characterization of dendrimer-functionalized mesoporous hydroxyapatite," ***Langmuir : the ACS Journal of Surfaces and Colloids***, Vol. 28, No. 39, (2012), 14018–14027.
23. J. E. L. Buddy D. Ratner, Allan S. Hoffman, Frederick J. Schoen, Biomaterials Science An Introduction to Materials in Medicine, Third edit. ***Elsevier Ltd***, (2013), 139-160.
24. S. E. Anachkov, K. D. Danov, E. S. Basheva, P. A. Kralchevsky, and K. P. Ananthapadmanabhan, "Determination of the aggregation number and charge of ionic surfactant micelles from the stepwise thinning of foam films," ***Advances in Colloid and Interface Science***, Vol. 183, (2012), 55–67.
25. Y. S. Lee, Self-assembly and nanotechnology: a force balance approach. ***John Wiley & Sons***, (2008), 59-60.
26. Y. V Kazakevich and R. Lobrutto, HPLC for pharmaceutical scientists. ***John Wiley & Sons***, (2007), 176.
27. H. Chen, T. Hu, X. Zhang, K. Huo, P. K. Chu, and J. He, "One-step synthesis of monodisperse and hierarchically mesostructured silica particles with a thin shell.," ***Langmuir***, Vol. 26, No. 16, (2010), 13556–13563.
28. J. L. Burgot, Ionic equilibria in analytical chemistry. ***Springer***, (2012), 58.

Effect of Micellization pH on Properties of Sphere-like Mesoporous Hydroxyappatite

L. Bakhtiari[a], H. R. Rezaie[a], J. Javadpour[a], M. Erfan[b], M. A. Shokrgozar[c]

[a]*School of Metallurgical and Materials Engineering, Iran University of Science and Technology, Tehran, Narmak , Iran.*
[b]*School of Pharmacy, Shahid Beheshti University of Medical Sciences, Tehran, Iran.*
[c]*National Cell Bank of Iran, Pasteur Institute of Iran, Tehran, Iran*

P A P E R I N F O

Paper history:
Received 19 November 2014
Received in revised form 09 June 2015
Accepted 11 June 2015

Keywords:
Mesoporous
Hydroxy Appatite
Micellization pH
Sphere-like

چکیده

هیدروکسی آپاتیت مزوپور به کمک روش خود چینشی با استفاده از ماده فعال سطحی کاتیونی سی تب (CTAB) و ۱- دودکانتول به عنوان عامل تورم زا با نسبت جرمی عامل تورم زا/ماده فعال سطحی برابر ٤/۲۲ و دمای سنتز ۸۰ °C در pH های متفاوت میسلیزاسیون سنتز شد. نتایج آنالیزهای میکروسکوپ الکترونی روبشی (FESEM)، پراش پرتو ایکس (XRD)، سطح ویژه (BET)، حجم تخلخل (به روش BJH)، اسپکتروسکوپی مادون قرمز (FTIR) و پراش پرتو ایکس زاویه پایین (LA-XRD) در کنار نتایج تیتراسیون ۱-دودکانتول نشان داد که تغییرات pH میسلیزاسیون به میزان ۱ واحد به صورت نمایی برای ۱-دودکانتیول یونیزه شده تغییر می کند. pH میسلیزاسیون نقش اساسی در خواص فیزیکی- شیمیایی نمونه ها دارد. به عبارت دیگر افزایش pH باعث افزایش درجه یونیزاسیون عامل تورم زا شده و با افزایش میزان ۱-دودکانتول یونیزه شده، تورم مایسل بیشتر شده و موجب افزایش سایز حفره می شود (سایز حفره ۲/۹۳ درpH پایین و ۲٤/٤۸ در pH بالا). تغییر در pH میسلیزاسیون همچنین روی ثابت دی الکتریک آب اثر گذاشته و منجر به تغییر در سایز ذرات نهایی می شود.

.***doi**: 10.5829/idosi.ije.2015.28.07a.13*